Boosting Hyperalignment Performance with Age-specific Templates

Yuqi Zhang
Dartmouth College

Maria Ida Gobbini
University of Bologna

James V. Haxby*
Dartmouth College

Ma Feilong*
Dartmouth College

*: These authors contributed equally.

Abstract

Hyperalignment aligns individual brain activity and functional connectivity patterns to a common, high-dimensional model space, resolving idiosyncrasies in functional–anatomical correspondence and revealing shared information encoded in fine-grained spatial patterns. Given that the brain undergoes significant developmental and functional changes over the lifespan, it is likely that certain features in brain functional organization are more prominent in certain age groups than others. In this study, we examined whether age-specific functional templates, as compared to a canonical template, could enhance alignment accuracy across diverse age groups. We used the Cambridge Centre for Ageing and Neuroscience (Cam-CAN) dataset (18 to 87 yo) to build age-specific templates and tested their performance for analyzing data in young and old brains in both the Cam-CAN dataset and the Dallas Lifespan Brain Study (DLBS) dataset (20 to 90 yo). We found the congruent age-specific template outperforms the incongruent template for various analyses, including inter-subject correlation of hyperaligned connectivity profiles and predicting individualized connectomes using the template. The results are consistent across both datasets. This work enhances our understanding of age-related differences in brain function, highlights the benefits of creating age-specific templates to refine hyperalignment model performance, and may contribute to the development of age-sensitive diagnostic tools and interventions for neurological disorders.

Keywords: fMRI, hyperalignment, brain aging, individual differences, functional connectivity

Introduction

Information encoded in the cortex can be decoded from fine-grained patterns of cortical activity via multivariate pattern analysis of fMRI data (Haxby et al., 2001, 2014). However, there is considerable variability across individual brains when encoding the same information (Cox & Savoy, 2003). Traditional approaches to brain alignment often fail to capture the fine-grained functional correspondence between brains due to topographic variability. Hyperalignment is a computational approach for modeling how the brain encodes shared information across individuals, despite individual variability in cortical topographies (Haxby et al., 2011, 2020). The hyperalignment model built upon human connectome (connectivity hyperalignment, CHA) captures both coarse- and fine-scale structure of connectivity shared across brains (Guntupalli et al., 2018). This approach also enhances the reliability of individual differences by affording analysis of differences in the fine-grained structure of the functional connectome (Feilong et al., 2018, 2021).

The performance of hyperalignment models in human connectomics may be significantly influenced by the age of the individuals used to build the templates. Given that the brain undergoes substantial developmental, structural, and functional changes across the lifespan, age-related variations can impact the alignment of neural data across individuals. In this study, we investigate whether the incorporation of age-specific templates enhances the performance of hyperalignment models. Examining this aspect could not only improve hyperalignment accuracy across diverse age groups but also inform age-sensitive intervention strategies. Individual differences in the brain arise from both aging and neurological diseases and brain injuries. This knowledge also could open new pathways for creating more effective diagnostic tools for neurological disorders.

We investigated the problem by developing age-specific hyperalignment templates and analyzing both the average inter-subject correlation of connectomes in the common model space and prediction accuracy on individual connectomes in participants' native spaces, using two distinct publicly-available lifespan datasets, the Cambridge Centre for Ageing and Neuroscience (Cam-CAN) dataset and the Dallas Lifespan Brain Study (DLBS) dataset. The results indicate that congruent templates (i.e., constructed using data from the same age group) enhance ISC of connectomes and prediction accuracy of individual connectomes compared to incongruent templates.

Methods

Datasets

We used two datasets that vary substantially in participant age for our analysis, namely the Cam-CAN dataset and the DLBS dataset. We built age-specific templates using the Cam-CAN dataset and evaluated their performance using both the Cam-CAN dataset and the DLBS dataset.

Cambridge Centre for Ageing and Neuroscience (Cam-CAN)

The Cambridge Centre for Ageing and Neuroscience (Cam-CAN) dataset comprises fMRI data of over 600 people from a cross-sectional adult lifespan (18 to 87 years old) population-based sample, with approximately 25 minutes of fMRI data per individual (Taylor et al., 2017). All MRI datasets were collected at MRC-CBSU using a 3T Siemens TIM Trio Scanner with a 32-channel head coil, 3.0 × 3.0 × 4.44 mm^3 voxels and 20% gap. Each individual's fMRI data were collected during three different tasks: 1) 8 minutes 40 seconds of resting state with eyes closed ('rest'); 2) 8 minutes of movie-watching of the film "Bang! You're dead" ('bang'); 3) 8 minutes 40 seconds of sensorimotor task ('smt') during which participants were asked to press a button upon the presentation of a visual and/or auditory stimulus. Both resting state and the sensorimotor task used single echo sequences with TR = 1970 ms, TE = 30 ms, flip angle = 78°, and the movie-watching task used multi-echo sequences with TR = 2470 ms, TEs = 9.4, 21.2, 33, 45, 57 ms, flip angle = 78°. There are 646 people that have the full records of all three functional scans (age distribution shown in Table 1).

Table 1. Age group division and corresponding training/test set sizes

			Cam-CAN		DLBS
Age Group	Age Range	Number of Participants	Training Group	Test Group	Test Group
Young	18 - 45	215	144	71	92
Old	65 - 90	216	144	72	182

Dallas Lifespan Brain Study (DLBS)

The Dallas Lifespan Brain Study (DLBS) dataset collects multi-modal data from over 400 individuals across the entire adult lifespan, ranging from 20 to 90 years old. The dataset contains longitudinal data from multiple scan sessions conducted over 10 years. In this study, we focused on the fMRI data

from the first and most complete scan session, which was collected between 2008 and 2014 from 464 participants. The fMRI data were collected using a Philips Achieva 3T scanner at the University of Texas Southwestern Medical Center, with 3.4 × 3.4 × 3.5 mm^3 voxels, TR = 2000 ms, TE = 25 ms, flip angle = 80° (Chan et al., 2014; Chen et al., 2021; Kennedy et al., 2015; Park et al., 2012). Among these participants, 407 completed a scanning session that included: 1) 7 minutes and 56 seconds of the words task, during which participants were shown 128 words and asked to make a semantic judgment on whether each word represented something living or nonliving; 2) three runs of 5 minutes and 56 seconds each of the scenes task, where participants were presented with outdoor landscape scenes and had to determine whether water was present in each scene; and 3) 6 minutes and 14 seconds of resting state. Among the 407 selected participants, 92 were younger than 45 years old, 133 were between 45 and 65 years old, and 182 were older than 65 years old.

Preprocessing

We preprocessed all MRI data using fMRIPrep (Esteban et al., 2019), with version 20.2.7 for the Cam-CAN dataset, and version 24.1.0 for the DLBS dataset. For each participant, the cortical surface was reconstructed using the high-resolution structural scans. The functional data were corrected for head motion, projected onto the cortical surface model, and resampled to the onavg-ico32 cortical surface template, which uniformly samples different parts of the cortex (Feilong et al., 2024). After that, we used linear regression to partial out nuisance regressors from our data. The list of nuisance regressors includes 6 head motion parameters and their derivatives, framewise displacement, global signal, 6 aCompCor components from cerebrospinal fluid and white matter, and polynomial trends up to the 2nd order. After the regression, we normalized the time series of each cortical vertex to zero mean and unit variance.

Individual connectome calculation

We computed two kinds of connectomes for each of the two datasets based on different functional scans: (a) using both Cam-CAN resting state and sensorimotor task data, (b) using Cam-CAN movie-watching data, (c) using DLBS resting state and words task data, and (d) using DLBS scenes task data. For each individual and each task, we downsampled the data matrix from 'onavg-ico32' space (19341 vertices) to 'onavg-ico8' space (1210 vertices) and used the downsampled data as connectivity targets. For each of the 19341 cortical vertices, we computed its connectivity profile as its correlations with the 1210 connectivity targets and z-scored the connectivity profile. The 19341 connectivity profiles collectively form the connectome matrix of the individual and task.

Hyperalignment template creation

We classified the participants into three different age groups—young, mid, and old—with each group consisting of around the same number of people. Our analyses focus on the young and old groups (Table 1)

For each age group, we built 10 distinct templates by randomly dividing the participants into a training group to build the template, and a test group to examine template performance. The number of participants used to build the template was two thirds of the minimum number of participants among different age groups. Each template was created using a searchlight-based algorithm with a 20 mm searchlight radius, based on the training group participants' connectome data (1210 × 19341 per individual) calculated from the resting state data and sensorimotor task data. Then we calculated individual hyperalignment transformation matrices (R) by hyperaligning test participants' individual connectomes to the template (Figure 1). In practice, we computed the templates and transformations separately for each hemisphere, which does not affect any results. Given functional connectomes might differ across tasks, for each template based on resting state and sensorimotor data, we computed a corresponding template based on the movie-viewing data, which was used in the analysis of predicting individual connectomes as described below.

Inter-subject correlation (ISC)

We computed the inter-subject correlation (ISC) of connectivity profiles in the common model space to evaluate template performance, where higher ISCs indicate better performance. For each participant in

the test set, we computed the participant's hyperalignment transformation matrix (R) using the connectome based on resting state and sensorimotor task data, and applied the transformation matrix to the original movie-watching responses to compute the hyperaligned connectome. This ensures that the data used to compute hyperalignment transformation are independent from the data used to evaluate performance. We computed ISC as the correlation between the participant's connectivity profile and the average profile across other test participants in the same age group (Figure 1). Each participant has up to 20 ISC maps (10 young templates and 10 old templates), and we averaged ISC maps of the same kind (young or old) for each participant. When we averaged *r* values, we converted them to *z* values (Fisher transform), averaged the *z* values, and converted them back to *r* values. Based on the analysis, we either averaged them across cortical vertices (Figures 2a, 2b, 3a, 3b) or participants of the same age group (Figures 2c, 3c).

Predicting individual connectome

To test whether the age-specific template captures more age-specific information, we evaluated its ability to predict the connectomes of held-out test participants (Figure 1). We derived each participant's predicted movie-viewing connectome as the matrix multiplication of the movie-viewing template and the transpose of the individual's transformation matrix (R^T, derived from resting state and sensorimotor task data). We then compared the predicted connectome with the participant's actual movie-viewing connectome based on the correlation of the corresponding connectivity profiles in these two connectomes.

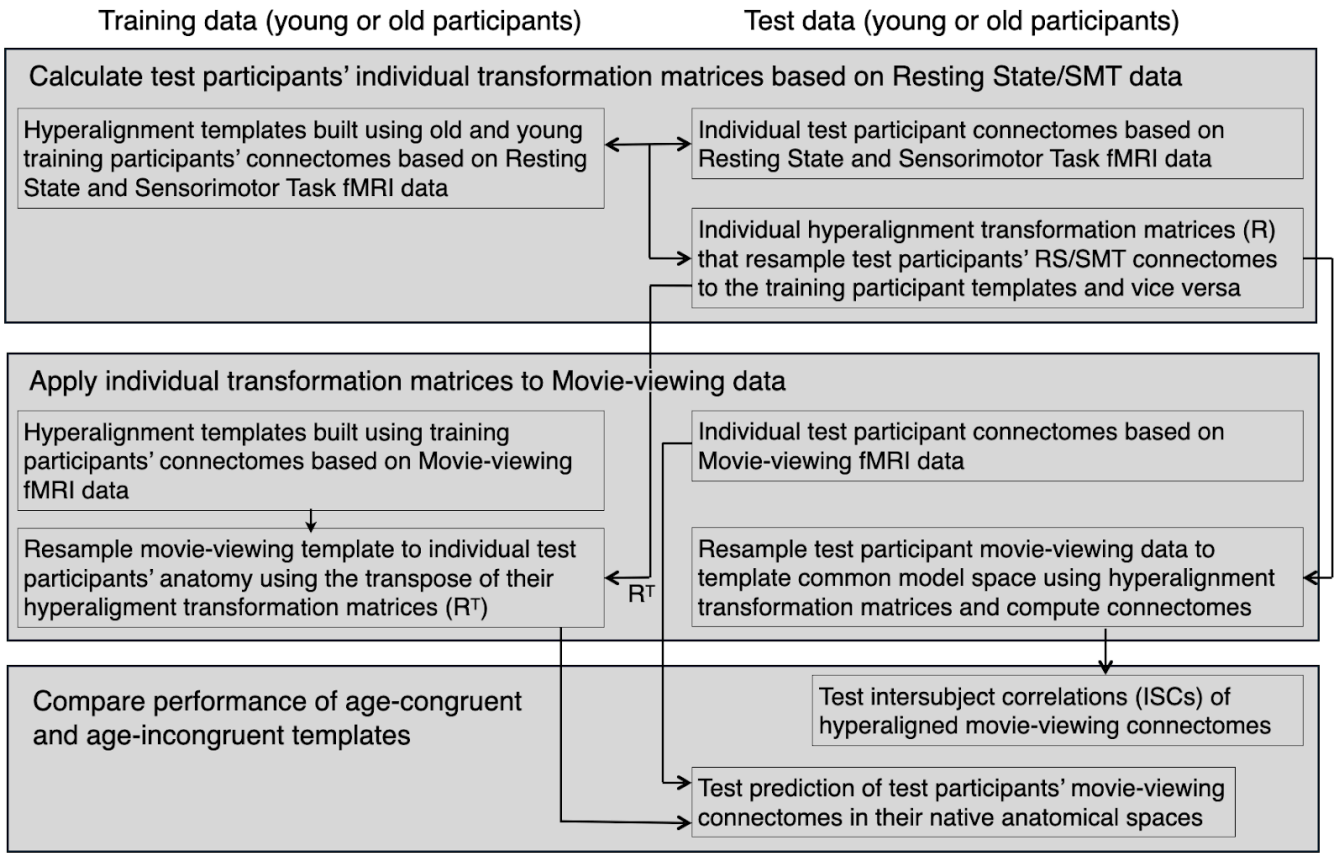

Figure 1: Schematic of the procedure for building hyperalignment templates

Results

We evaluated the performance of the templates using two metrics: (a) ISC of functional connectivity in the common template space, where higher ISCs indicate better alignment of connectivity in the template space; and (b) similarity between model-predicted and measured connectomes in each participant's native anatomical space, where higher similarity suggests the template contains more relevant information and better predicts individualized connectomes. Across both datasets and both metrics, we found that congruent age-specific templates outperformed incongruent templates.

Inter-subject correlation (Cam-CAN)

We first evaluated the performance of templates constructed from both young and old age groups on ISCs of connectomes in the common model template space. We computed the z-difference (difference in Fisher z transformed correlations) between post-alignment ISC values derived from congruent and incongruent templates (Figure 2a). Hyperalignment based on congruent age-specific templates yields higher ISCs in both age groups, with a more pronounced effect in the young group. Breaking down the data by participant, we found that most participants (97.6% in the young group, 74.2% in the old group) exhibited higher ISCs when comparing the results for congruent and incongruent templates (Figure 2b). The topography of mean ISC differences displayed in Figure 2c illustrate that congruent templates perform better in the frontal, temporal, and parietal lobes.

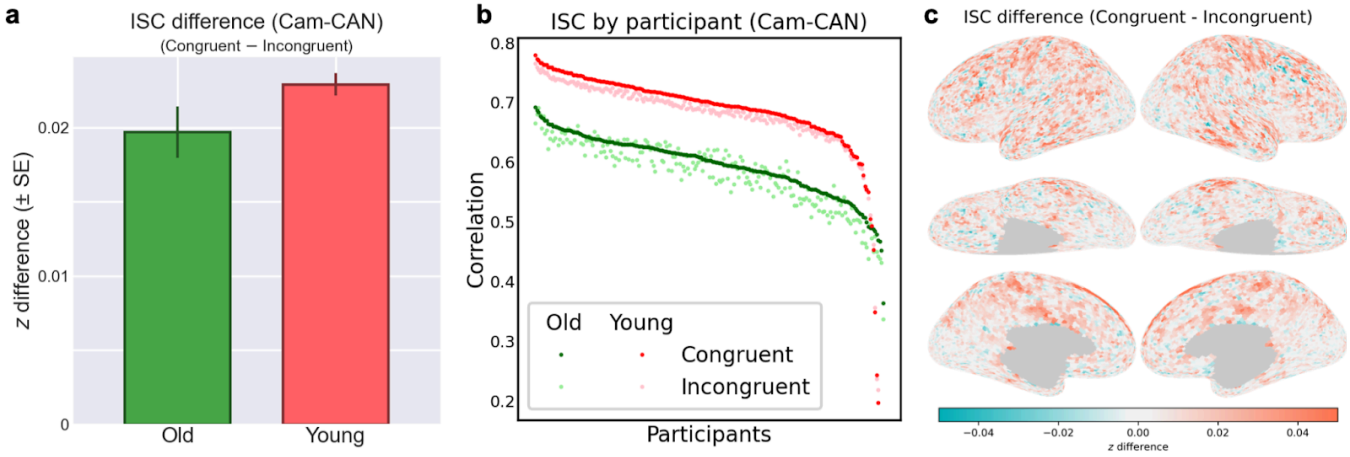

Figure 2: Inter-subject Correlation Results (Cam-CAN). (a) The average ISC difference across all participants in the old group is 0.0197 ± 0.0017 and in the young group is 0.0229 ± 0.0008. (b) Scatter plot of each participant's average ISC value derived from different congruent and incongruent templates. (c) Topographic distribution of ISC difference across different brain regions.

Inter-subject correlation (DLBS)

The results based on the Cam-CAN dataset demonstrates that hyperalignment templates from the same age group work better, and this effect generalizes across tasks (from resting state and sensorimotor to movie-watching) and scan protocols (single-echo sequence to multi-echo sequence). In this analysis, we use the DLBS dataset, which was collected with a different scanner, different group of participants, and different tasks, to further test the generalizability of our results.

We applied the hyperalignment templates—constructed using Cam-CAN data from the two age groups (young and old)—to the DLBS dataset. Since the two datasets do not share identical functional tasks, we calculated transformation matrices that resample the resting state and words task fMRI data of the DLBS dataset into the Cam-CAN templates for young and old

participants. We then applied the transformation matrices to connectomes based on the scenes task data and calculated the ISCs. The ISC results align well with those from the Cam-CAN dataset (Figure 3). We observed a statistically significant difference between ISC values derived from congruent and incongruent templates in both age groups (Figure 3a). Although the differences among individual participants were smaller than those in the Cam-CAN dataset, they were still evident (Figure 3b, 92.4% participants in the young group and 57.7% participants in the old group have higher congruent ISC values). SImilar to the results with the Cam-CAN data, we noted a stronger effect of template on ISCs in the parietal, temporal, and occipital cortices (Figure 3c).

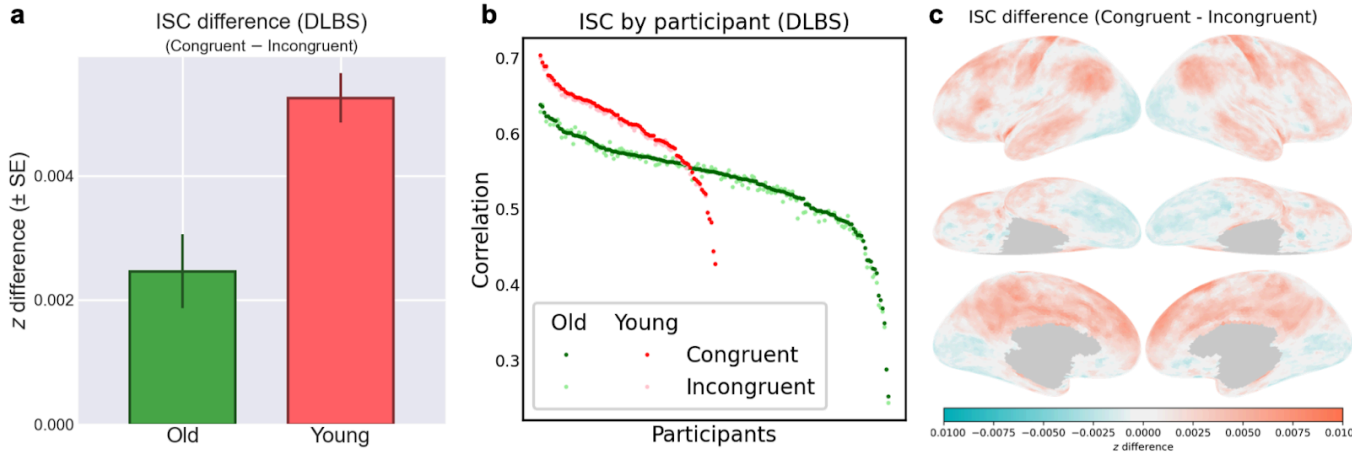

Figure 3: Inter-subject Correlation Results (DLBS). (a) The average ISC difference across all participants in the old group is 0.0025 ± 0.0006 and in the young group is 0.005 ± 0.0004. (b) Scatter plot of each participant's average ISC value derived from different congruent and incongruent templates. (c) Topographic distribution of ISC difference across different brain regions

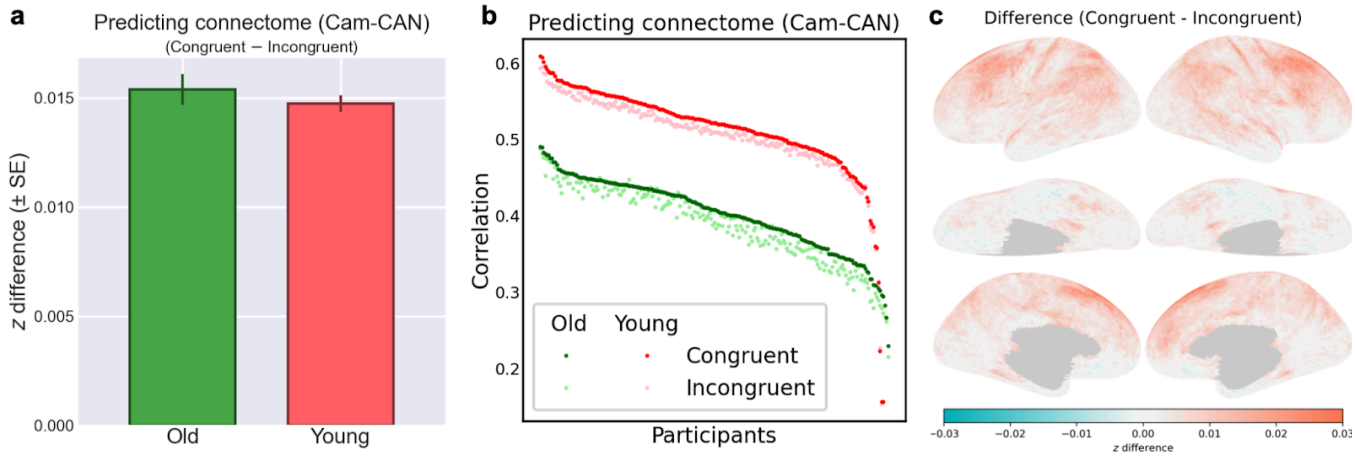

Figure 4: Prediction performance comparison between congruent and incongruent templates. (a) The average correlation difference across all participants in the old group is 0.0154 ± 0.0007 and in the young group is 0.0147 ± 0.0004. (b) Scatter plot of each participant's average correlation value derived from different congruent and incongruent templates. (c) Topographic correlation difference across different brain regions.

Predicting connectomes (Cam-CAN)

Higher ISCs can arise from both (a) better alignment across participants and (b) filtering out noise during hyperalignment transformations. Though it is unlikely that our ISC results were driven by reduced noise, to rule out the possibility, we assessed how well

different templates predict each participant's connectome, where the prediction performance is not influenced by filtering effects.

For each individual, we calculated the correlation between the predicted connectome, generated using different age group hyperalignment templates, and the actual connectome, calculated using movie watching fMRI data. A higher correlation indicates a more accurate prediction, which means better performance of the hyperalignment template.

We compared the performance of congruent templates (built from the same age group) and incongruent templates (built from a different age group) on Cam-CAN participants. For each participant in the test sets of both age groups, we calculated the predicted connectome using 20 templates—10 from each age group. We then computed the correlation for each participant and averaged the individual results across templates in the same age group. Figure 4a shows the z-difference between correlations calculated using congruent and incongruent templates for each participant in both groups. The results clearly indicate that predictions using congruent templates are more accurate than those using incongruent templates, with the older group demonstrating a slightly stronger impact. Examining the participant breakdown in Figure 4b, we observed that almost all participants (98.6% in the young group and 94.4% in the old group) have a better connectome prediction using congruent templates than using incongruent templates from the other group. The topographic distribution of mean differences between the predicted connectomes using congruent and incongruent templates are displayed in Figure 4c. Congruent templates generally perform better in the frontal and parietal lobes—regions primarily responsible for cognitive functions—which can be significantly influenced by age.

To evaluate the influence of age on the performance of hyperalignment template across the entire lifespan, we computed the correlation between actual connectome and predicted connectome of all participants using both young templates and old templates. As an individual's age becomes more distant from the template age group, the relative performance of the template decreases (Figure 5a, 5b). This result indicates that the more congruent the template age group is with the participant's age, the more accurate the prediction becomes.

Overall, congruent age-specific templates better predict participants' connectomes than incongruent templates. As the participant's age diverges further from the template age group, the prediction accuracy gets worse. This result indicates that age independent templates are necessary for improving the performance of hyperalignment.

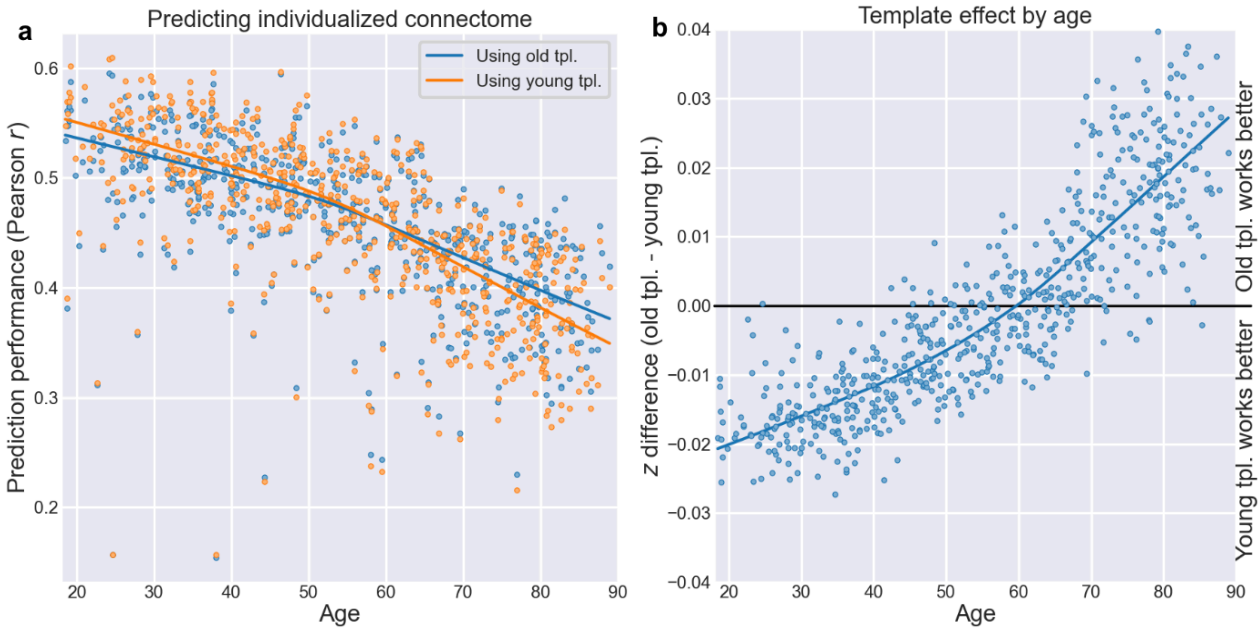

Figure 5: Comparison of individual connectome prediction across all age spans. (a) Scatter plot showing Pearson correlation between actual connectome and predicted connectome derived from young and old templates for individuals across all age spans (b) Correlation difference among individuals between two age group templates, ordered by age.

Discussion

In this paper, we analyzed the effect of age on hyperalignment performance. Our findings demonstrate the significant impact of age-specific hyperalignment templates on the accuracy of individualized connectome prediction, as well as the inter-subject correlation (ISC) values after hyperalignment.

Our results show that congruent hyperalignment templates—those aligned with the participant's age group—consistently achieved higher correlation between predicted individual connectomes and actual connectomes compared to incongruent templates. When predicting an individual's connectome in different age groups using either old group templates (> 65 years old) or young group templates (< 45 years old), as the individual's age becomes more distant from the template age group, the prediction accuracy drops, and the difference between congruent and incongruent template prediction increases.

The ISC results on both Cam-CAN and DLBS datasets further validate the age effect on hyperalignment template performance. Average ISC values calculated using both datasets are higher when projecting individual connectome to the common model space derived from congruent age group templates rather than incongruent age group templates.

The performance of hyperalignment templates probably could be significantly enhanced with access to more fMRI data. Previous hyperalignment study shows that the more data used in building the templates for estimating individual tuning matrices, the better the model performs (Feilong et al., 2023). Currently, the templates are built using only approximately 16 minutes of fMRI functional data from around 200 participants. We expect that better and more stable model performance could be achieved by incorporating data from more participants and increasing the amount of data to at least 1 hour per participant. Moreover, incorporating data from a variety of functional tasks into the template construction process might provide additional information that could enhance template performance as currently our templates are constructed using only resting state and sensorimotor task data. With increased data collection and including data from a broader range of functional tasks, we could capture a broader range of neural activities and idiosyncrasies, potentially leading to more robust and flexible hyperalignment templates and a more precise and reliable alignment between individual connectomes and the common model space.

In this work, we only focused on the impact of age on hyperalignment templates and observed a significant improvement using congruent age templates compared to incongruent ones. Congruent age templates may provide more sensitive study of the effect of age-related diseases, such as Alzheimer's disease and Parkinson's disease, on functional brain organization. Our results further suggest that it may be fruitful to develop separate hyperalignment templates for distinct populations characterized by different neurological or psychiatric diseases. Just as age introduces specific variations in neural architecture, various diseases produce unique alterations in brain structure and function. By constructing disease-specific templates, it may be possible to capture these distinctive neural patterns with greater accuracy, leading to more precise alignment of individual connectomes. This approach could provide insights into the pathophysiological mechanisms underlying various clinical conditions and broaden the use of hyperalignment models in clinical neuroscience.

References

Chan, M. Y., Park, D. C., Savalia, N. K., Petersen, S. E., & Wig, G. S. (2014). Decreased segregation of brain systems across the healthy adult lifespan. *Proceedings of the National Academy of Sciences*, *111*(46), E4997–E5006.

https://doi.org/10.1073/pnas.1415122111

Chen, X., Farrell, M. E., Rundle, M. M., Chan, M. Y., Moore, W., Wig, G. S., & Park, D. C. (2021). The relationship of functional hippocampal activity, amyloid deposition, and longitudinal memory decline to memory complaints in cognitively healthy older adults. *Neurobiology of Aging*, *105*, 318–326. https://doi.org/10.1016/j.neurobiolaging.2021.04.020

Cox, D. D., & Savoy, R. L. (2003). Functional magnetic resonance imaging (fMRI) "brain reading": Detecting and classifying distributed patterns of fMRI activity in human visual cortex. *NeuroImage*, *19*(2 Pt 1), 261–270. https://doi.org/10.1016/s1053-8119(03)00049-1

Esteban, O., Markiewicz, C. J., Blair, R. W., Moodie, C. A., Isik, A. I., Erramuzpe, A., Kent, J. D., Goncalves, M., DuPre, E., Snyder, M., Oya, H., Ghosh, S. S., Wright, J., Durnez, J., Poldrack, R. A., & Gorgolewski, K. J. (2019). fMRIPrep: A robust preprocessing pipeline for functional MRI. *Nature Methods*, *16*(1), 111–116. https://doi.org/10.1038/s41592-018-0235-4

Feilong, M., Guntupalli, J. S., & Haxby, J. V. (2021). The neural basis of intelligence in fine-grained cortical topographies. *eLife*, *10*, e64058. https://doi.org/10.7554/eLife.64058

Feilong, M., Jiahui, G., Gobbini, M. I., & Haxby, J. V. (2024). A cortical surface template for human neuroscience. *Nature Methods*, *21*(9), 1736–1742. https://doi.org/10.1038/s41592-024-02346-y

Feilong, M., Nastase, S. A., Guntupalli, J. S., & Haxby, J. V. (2018). Reliable individual differences in fine-grained cortical functional architecture. *NeuroImage*, *183*, 375–386. https://doi.org/10.1016/j.neuroimage.2018.08.029

Feilong, M., Nastase, S. A., Jiahui, G., Halchenko, Y. O., Gobbini, M. I., & Haxby, J. V. (2023). The individualized neural tuning model: Precise and generalizable cartography of functional architecture in individual brains. *Imaging Neuroscience*, *1*, 1–34. https://doi.org/10.1162/imag_a_00032

Guntupalli, J. S., Feilong, M., & Haxby, J. V. (2018). A computational model of shared fine-scale structure in the human connectome. *PLOS Computational Biology*, *14*(4), e1006120. https://doi.org/10.1371/journal.pcbi.1006120

Haxby, J. V., Connolly, A. C., & Guntupalli, J. S. (2014). Decoding neural representational spaces using multivariate pattern analysis. *Annual Review of Neuroscience*, *37*, 435–456. https://doi.org/10.1146/annurev-neuro-062012-170325

Haxby, J. V., Gobbini, M. I., Furey, M. L., Ishai, A., Schouten, J. L., & Pietrini, P. (2001). Distributed and Overlapping Representations of Faces and Objects in Ventral Temporal Cortex. *Science*, *293*(5539), 2425–2430. https://doi.org/10.1126/science.1063736

Haxby, J. V., Guntupalli, J. S., Connolly, A. C., Halchenko, Y. O., Conroy, B. R., Gobbini, M. I., Hanke, M., & Ramadge, P. J. (2011). A common, high-dimensional model of the representational space in human ventral temporal cortex. *Neuron*, *72*(2), 404–416. https://doi.org/10.1016/j.neuron.2011.08.026

Haxby, J. V., Guntupalli, J. S., Nastase, S. A., & Feilong, M. (2020). Hyperalignment: Modeling shared information encoded in idiosyncratic cortical topographies. *eLife*, *9*, e56601. https://doi.org/10.7554/eLife.56601

Kennedy, K. M., Rodrigue, K. M., Bischof, G. N., Hebrank, A. C., Reuter-Lorenz, P. A., & Park, D. C. (2015). Age trajectories of functional activation under conditions of low and high processing demands: An adult lifespan fMRI study of the aging brain. *NeuroImage*, *104*, 21–34. https://doi.org/10.1016/j.neuroimage.2014.09.056

Park, J., Carp, J., Kennedy, K. M., Rodrigue, K. M., Bischof, G. N., Huang, C.-M., Rieck, J. R., Polk, T. A., & Park, D. C. (2012). Neural Broadening or Neural Attenuation? Investigating Age-Related Dedifferentiation in the Face Network in a Large Lifespan Sample. *Journal of Neuroscience*, *32*(6), 2154–2158. https://doi.org/10.1523/JNEUROSCI.4494-11.2012

Taylor, J. R., Williams, N., Cusack, R., Auer, T., Shafto, M. A., Dixon, M., Tyler, L. K., Cam-CAN, & Henson, R. N. (2017). The Cambridge Centre for Ageing and Neuroscience (Cam-CAN) data repository: Structural and functional MRI, MEG, and cognitive data from a cross-sectional adult lifespan sample. *NeuroImage*, *144*, 262–269. https://doi.org/10.1016/j.neuroimage.2015.09.018